


 Cite this: *RSC Adv.*, 2021, **11**, 8033

N-type and p-type molecular doping on monolayer MoS₂†

 Ong Kim Le,^{ab} Viorel Chihai, ^c Vo Van On^d and Do Ngoc Son ^{*ab}

Monolayer MoS₂ has attracted much attention due to its high on/off current ratio, transparency, and suitability for optoelectronic devices. Surface doping by molecular adsorption has proven to be an effective method to facilitate the usage of MoS₂. However, there are no works available to systematically clarify the effects of the adsorption of F₄TCNQ, PTCDA, and tetracene on the electronic and optical properties of the material. Therefore, this work elucidated the problem by using density functional theory calculations. We found that the adsorption of F₄TCNQ and PTCDA turns MoS₂ into a p-type semiconductor, while the tetracene converts MoS₂ into an n-type semiconductor. The occurrence of a new energy level in the conduction band for F₄TCNQ and PTCDA and the valence band for tetracene reduces the bandgap of the monolayer MoS₂. Besides, the MoS₂/F₄TCNQ and MoS₂/PTCDA systems exhibit an auxiliary optical peak at the long wavelengths of 950 and 850 nm, respectively. Contrastingly, the MoS₂/tetracene modifies the optical spectrum of the monolayer MoS₂ only in the ultraviolet region. The findings are in good agreement with the experiments.

Received 29th November 2020

Accepted 15th February 2021

DOI: 10.1039/d0ra10075g

rsc.li/rsc-advances

1. Introduction

The monolayer MoS₂ is a semiconducting transition metal dichalcogenide with an optical bandgap of about 1.8 eV. This material has proven to possess high on/off current ratio and transparency, making it suitable for electronic and optoelectronic applications.^{1,2} The properties of monolayer MoS₂ are adjustable by modifying the crystal structure, doping with different elements, and the adsorption of organic molecules.^{3–6} The application of organic molecular adsorption is attractive because of advantages such as mechanical flexibility, easy fabrication, light weight, and low cost.^{7,8} Organic molecular adsorption has been demonstrated as a viable method to optimize material properties,⁶ also to protect MoS₂ from oxidation under ambient conditions.⁹ Therefore, it is essential to understand the behavior of the organic adsorption on the monolayer MoS₂ to optimize its performance for optoelectronic uses.

Here, we studied the adsorption of three organic molecules, *i.e.*, 2,3,5,6-tetrafluoro-7,7,8,8-tetracyanoquinodimethane

(F₄TCNQ), perylene-3,4,9,10-tetracarboxylic dianhydride (PTCDA), and tetracene. Where, F₄TCNQ is one of the most effective p-type dopants due to its strong ability of electron acceptance.^{10–13} The experiment showed that F₄TCNQ could modify the electrical and optical properties of MoS₂.¹¹ Hu *et al.* confirmed that the deposition of F₄TCNQ on the monolayer MoS₂ allows convenient control of the radioactive exciton recombination for laser and LED applications.¹² The charge transfer within the F₄TCNQ–MoS₂ interface can tune electrical and gas sensing properties.¹³ PTCDA and tetracene are popular organic semiconductors that have attracted many research interests in the past decades.^{8,14–19} Tetracene was used for field-effect transistors.^{20,21} The study of Habib showed the outstanding luminescent properties of the MoS₂/PTCDA system.¹⁷ Also, Wang *et al.* have demonstrated the novel MoS₂/PTCDA hybrid heterojunction synapse transistor with both electrical and optical modulation and efficient gate tunability.¹⁸ Besides, the MoS₂/tetracene is a good candidate for the anti-ambipolar field-effect transistor.²¹

The literature review showed that most of the available research is experiments, and there is no theoretical study available to elucidate the interaction between the MoS₂ monolayer and the mentioned organic molecules. Therefore, this work is going to clarify it by using the density functional theory (DFT) method and analyzing the electronic structure and optical properties of MoS₂ without and with the adsorption of F₄TCNQ, PTCDA, and tetracene. Furthermore, this work also considers the influences of pressure on the properties.

^aHo Chi Minh City University of Technology (HCMUT), Ho Chi Minh City, Vietnam. E-mail: dnson@hcmut.edu.vn

^bVietnam National University, Ho Chi Minh City, Vietnam

^cInstitute of Physical Chemistry “Ilie Murgulescu” of the Romanian Academy, Splaiul Independentei 202, Sector 6, 060021 Bucharest, Romania

^dInstitute of Applied Technology, Thu Dau Mot University, No. 6 Tran Van On Street, Phu Hoa Ward, Thu Dau Mot City, Binh Duong Province 75000, Vietnam

† Electronic supplementary information (ESI) available. See DOI: 10.1039/d0ra10075g



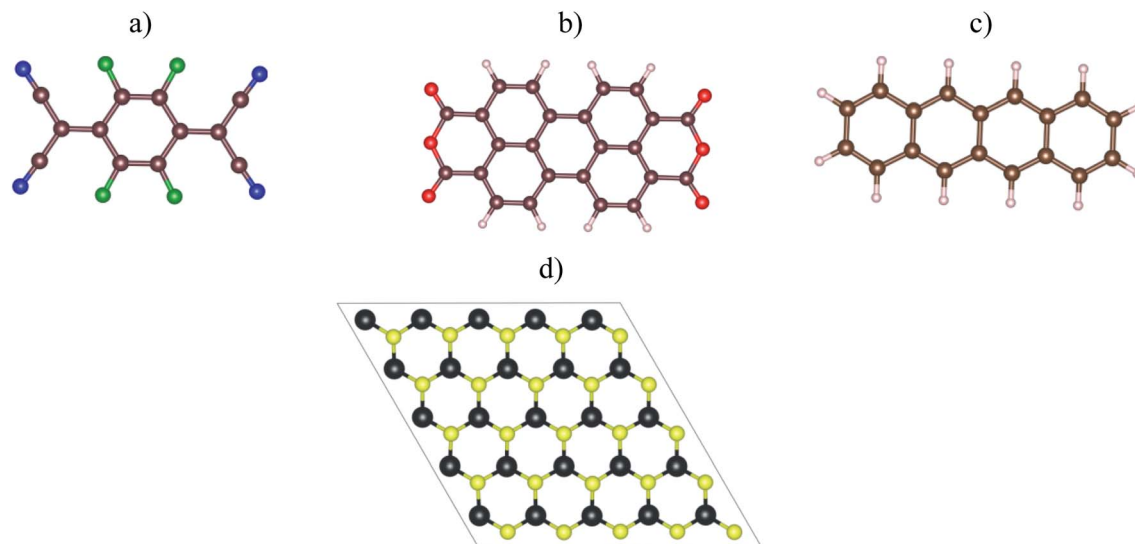


Fig. 1 The top view of organic molecules: (a) F_4TCNQ , (b) PTCDA, (c) tetracene, and (d) the monolayer MoS_2 . Blue (N), green (F), brown (C), red (O), white (H), yellow (S), and black (Mo).

2. Computational method

Fig. 1a–c visualized the molecular structure of F_4TCNQ ($C_{12}F_4N_4$), PTCDA ($C_{24}H_8O_6$), and tetracene ($C_{18}H_{12}$), respectively. The monolayer MoS_2 , shown in Fig. 1d, was described by a slab model with the 5×5 unit cell and a vacuum space of 27 \AA along the normal direction of the MoS_2 surface.

The optimized geometry structure and total energy of the monolayer MoS_2 with organic molecular adsorption were obtained with the aid of the Vienna *ab initio* simulation package (VASP).^{22–24} The projector-augmented-wave method was used to describe the valence electron–core ion interaction.^{25,26} The

electron exchange–correlation interactions were treated by using the PBE-GGA approximation of the Perdew–Burke–Ernzerhof,^{27,28} which has shown to be a reasonable approximation for the bandgap of the monolayer MoS_2 .²⁹ The plane-wave cutoff energy was 600 eV. The k -point mesh was sampled at $3 \times 3 \times 1$ in the first Brillouin zone by Monkhorst–Pack technique.³⁰ All atomic positions of MoS_2 and MoS_2 /organic-molecule systems are fully relaxed during the geometry optimization until the interatomic forces meeting the upper criterion of $0.001 \text{ eV \AA}^{-1}$.

The pressure applying to the system is defined by

$$P = \frac{E - E_0}{V - V_0}, \quad (1)$$

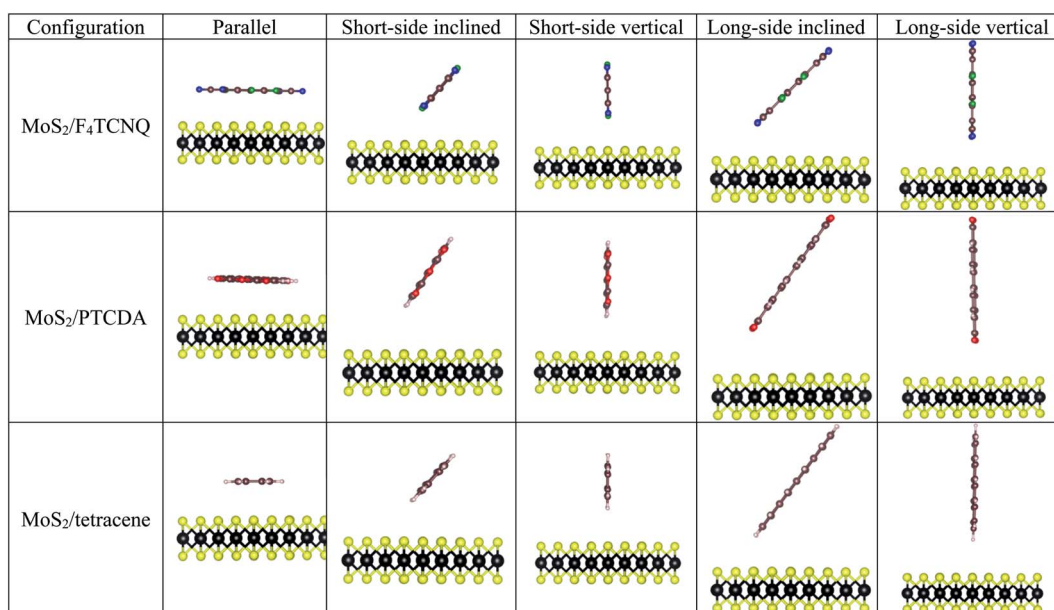


Fig. 2 The side view of the possible adsorption configurations of F_4TCNQ , PTCDA, and tetracene on the monolayer MoS_2 .



Table 1 Adsorption energy E_a (eV) for different configurations on the monolayer MoS₂ without strain

| Adsorption configuration | F ₄ TCNQ | PTCDA | Tetracene |
|--------------------------|---------------------|---------------|---------------|
| Parallel | -0.009 | 0.019 | 0.039 |
| Short-side inclined | -0.055 | -0.071 | -0.046 |
| Short-side vertical | -0.038 | -0.036 | -0.030 |
| Long-side inclined | -0.027 | -0.031 | -0.022 |
| Long-side vertical | -0.023 | -0.17 | 0.137 |

Table 2 Adsorption energy E_a and the shortest distance d from the organic molecule to the substrate surface

| a^a (Å) | MoS ₂ /F ₄ TCNQ | | MoS ₂ /PTCDA | | MoS ₂ /tetracene | |
|-----------|---------------------------------------|---------|-------------------------|---------|-----------------------------|---------|
| | E_a (eV) | d (Å) | E_a (eV) | d (Å) | E_a (eV) | d (Å) |
| 2.84 | 0.034 | 3.44 | 0.095 | 3.48 | 0.105 | 3.49 |
| 3.00 | 0.066 | 3.41 | 0.098 | 3.46 | 0.092 | 3.41 |
| 3.18 | -0.009 | 3.47 | 0.019 | 3.53 | 0.039 | 3.49 |
| 3.32 | -0.090 | 3.58 | -0.019 | 3.60 | -0.018 | 3.58 |
| 3.48 | -0.130 | 3.60 | -0.074 | 3.64 | -0.128 | 3.61 |
| 3.64 | -0.145 | 3.77 | -0.080 | 3.79 | -0.230 | 3.72 |

^a 2.84 and 3.00 Å: for compressive pressure; 3.18 Å: without pressure; 3.32, 3.48, and 3.64 Å: for tensile strain.

where, the energy and volume of the strained (unstrained) system are denoted as E and V (E_0 and V_0), respectively. The volume of the unit cell of the monolayer MoS₂ is $V = \frac{\sqrt{3}}{2}a^2c$ (a is the lattice constant and c is the thickness of the slab). The pressure is modified by changing the lattice constant $a = b$.

The adsorption energy of F₄TCNQ, PTCDA, and tetracene on the monolayer MoS₂ is calculated by

$$E_a = E_{\text{sub+om}} - (E_{\text{sub}} + E_{\text{om}}), \quad (2)$$

where, $E_{\text{sub+om}}$, E_{sub} , and E_{om} are the total energy of the MoS₂/organic molecule system, the isolated monolayer MoS₂, and the isolated organic molecule, respectively.

The optical property of the systems was determined through the imaginary part $\epsilon(\omega)$ of dielectric constant, which is calculated by the summation over empty states as follows:^{31,32}

$$\epsilon(\omega) = \frac{2\pi e^2}{V\epsilon_0} \sum_{k,v,c} |\langle \xi_k^c | \hat{v} \cdot r | \xi_k^v \rangle|^2 \delta[\hbar\omega - (E_k^v - E_k^c)], \quad (3)$$

here, ω is the frequency of emission, ϵ_0 is the dielectric constant of free space. The valence and conduction band wave functions are ξ_k^v and ξ_k^c , respectively. The unit cell volume is V , and the polarization vector of the electric field of the emission is \hat{v} .

3. Results and discussion

3.1. Structural properties

The optimized structural parameters for the monolayer MoS₂ were obtained in the previous publication,³³ where the optimized lattice constant was found to be $a = b = 3.18$ Å. To explore the adsorption properties of F₄TCNQ, PTCDA, and tetracene on the monolayer MoS₂, the geometry of the organic molecules with different configurations was optimized at several adsorption sites on the surface of MoS₂ as shown in Fig. 2. The most favorable adsorption of the F₄TCNQ, PTCDA, and tetracene molecules on the MoS₂ substrate was obtained for the short-side inclined configuration based on the most negative adsorption energy listed in Table 1.

Although the adsorption energy of the short-side inclined and parallel configurations are different, the electronic density of states (DOS) and the dielectric function are almost the same, as shown in Fig. S1 and S2 in the ESI.† Therefore, to make a comparison with the previous publication on polyethyleneimine,³³ we will perform a detailed analysis of the geometrical structure, the DOS, and the dielectric function for the parallel configuration of F₄TCNQ, PTCDA, and tetracene. Furthermore, we also found that the extension of the unit cell size to 6×6 and the inclusion of van der Waals correction (using vdW-DF functional) generated more negative adsorption energy (Tables S1 and S2†). However, the electronic structure of the MoS₂/F₄TCNQ, MoS₂/PTCDA, and MoS₂/tetracene systems remain the same as that of the unit cell 5×5 without van der Waals correction, as shown in Fig. S3.† Thus, it is acceptable to

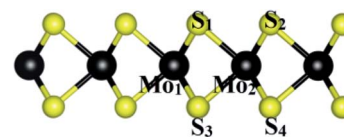


Fig. 4 The index of atoms for the bond lengths and angles.

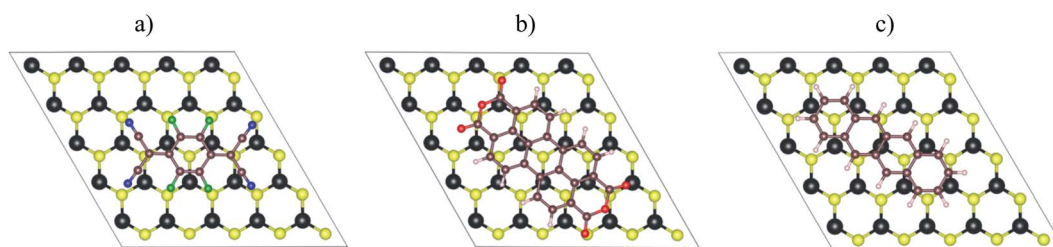


Fig. 3 The top view of the parallel adsorption configuration of the organic molecules on the monolayer MoS₂: (a) F₄TCNQ, (b) PTCDA, and (c) tetracene.



Table 3 Structural parameters of the MoS₂ substrate before and after the adsorption of the organic molecules. The index of atoms is described in Fig. 4

| Parameters | | MoS ₂ | MoS ₂ /F ₄ TCNQ | MoS ₂ /PTCDA | MoS ₂ /tetracene |
|------------|--|------------------|---------------------------------------|-------------------------|-----------------------------|
| Bonds (Å) | S ₁ -S ₂ | 3.183 | 3.160 | 3.162 | 3.160 |
| | S ₁ -S ₃ | 3.126 | 3.144 | 3.146 | 3.132 |
| | Mo ₁ -Mo ₂ | 3.187 | 3.183 | 3.180 | 3.182 |
| | Mo ₂ -S ₁ | 2.415 | 2.415 | 2.415 | 2.413 |
| Angles (°) | Mo ₁ S ₁ Mo ₂ | 82.30 | 82.46 | 82.34 | 82.52 |
| | S ₁ Mo ₂ S ₂ | 82.30 | 81.76 | 81.88 | 81.84 |
| | S ₁ Mo ₁ S ₃ | 80.54 | 80.90 | 81.02 | 80.78 |

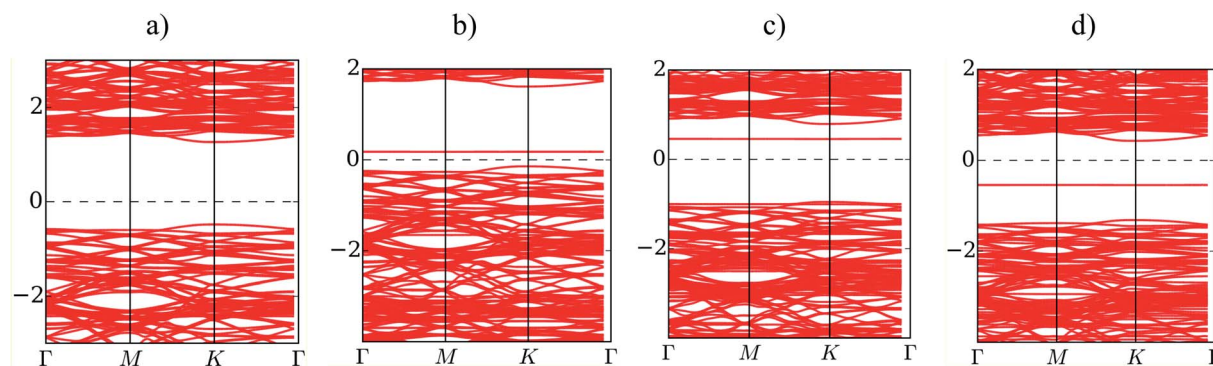


Fig. 5 The electronic band structure of (a) the monolayer MoS₂, (b) MoS₂/F₄TCNQ, (c) MoS₂/PTCDA, and (d) MoS₂/tetracene at zero pressure.

select the unit cell 5×5 and the PBE-GGA approximation in the present study.

Table 2 listed the adsorption energy and the vertical nearest distance to the MoS₂ surface of the F₄TCNQ, PTCDA, and tetracene molecules in the parallel configuration (Fig. 3). With the application of the tensile strain to the system, the organic molecules become stabilized with more negative adsorption energy relative to that at the lattice constant of 3.18 Å (without strain). The compressive pressure makes the molecules less stable with more positive adsorption energy. Table 2 also shows that the vertical nearest distance to the surface increases with the increase of the lattice constant. This result seems contradicted to the tendency of the more stable configuration of the adsorption upon modifying the tensile strain. Although the vertical nearest distance increases, the electrostatically attractive force between the adsorbates and MoS₂ increases at a faster rate.³³ Therefore, the adsorption energy becomes more negative. Besides, the interaction of the molecules with the surface is physisorption.

The geometrical parameters such as the bond length and bond angle of the MoS₂ substrate before and after the adsorption of the organic molecules are exhibited in Table 3. We found that the structural parameters did not change significantly after the adsorption of the molecules, which is consistent with the physical adsorption found in this work.

3.2. Electronic properties

Fig. 5 presents the band structure of MoS₂ before and after the adsorption of F₄TCNQ, PTCDA, and tetracene at zero pressure.

The bandgap is determined by the difference between the conduction band minimum and the valence band maximum. We find that the isolated substrate shows a direct bandgap of 1.68 eV at the K point, as listed in Table 4. The calculated bandgap of 1.68 eV comes from the electronic contribution only, while the experimental value of 1.80 eV has included the exciton binding energy.^{2,3,34} Upon the adsorption of the organic molecules, the new energy state occurs in the bandgap region of the MoS₂ substrate. The new energy level occurring above the Fermi level for the adsorption of F₄TCNQ and PTCDA implies that the substrate became the p-type semiconductor. Whilst, it occurring below the Fermi level for the adsorption of tetracene indicates that the monolayer MoS₂ became the n-type semiconductor. The existence of the new energy level shrinks the bandgap of the MoS₂ to 0.36, 1.43, and 0.72 eV for the

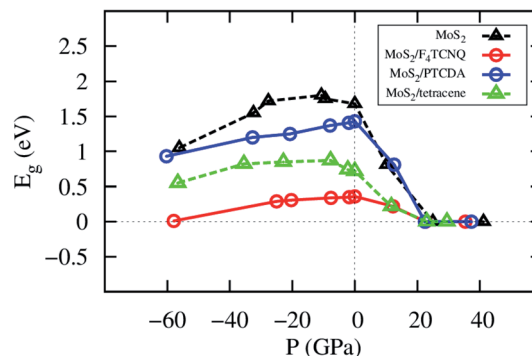


Fig. 6 The bandgap versus pressure of the monolayer MoS₂ with and without the adsorption of the organic molecules.



Table 4 The bandgap E_g of the monolayer MoS_2 with and without the adsorption of the organic molecules

| a (Å) | MoS_2^a | | $\text{MoS}_2/\text{F}_4\text{TCNQ}$ | | $\text{MoS}_2/\text{PTCDA}$ | | $\text{MoS}_2/\text{tetracene}$ | |
|---------|------------------|------------|--------------------------------------|------------|-----------------------------|------------|---------------------------------|------------|
| | P (GPa) | E_g (eV) | P (GPa) | E_g (eV) | P (GPa) | E_g (eV) | P (GPa) | E_g (eV) |
| 2.84 | -56.18 | 1.05 | -57.93 | 0.01 | -60.27 | 0.93 | -56.61 | 0.55 |
| 3.00 | -32.44 | 1.55 | -25.03 | 0.29 | -32.70 | 1.20 | -35.46 | 0.82 |
| 3.04 | -27.65 | 1.72 | -20.31 | 0.31 | -20.74 | 1.25 | -22.88 | 0.85 |
| 3.12 | -10.69 | 1.80 | -7.64 | 0.34 | -7.93 | 1.37 | -7.78 | 0.87 |
| 3.16 | -9.46 | 1.75 | -1.79 | 0.35 | -1.91 | 1.41 | -2.24 | 0.74 |
| 3.18 | 0 | 1.68 | 0 | 0.36 | 0 | 1.43 | 0 | 0.72 |
| 3.32 | 10.13 | 0.81 | 12.21 | 0.22 | 12.57 | 0.81 | 11.68 | 0.22 |
| 3.48 | 24.95 | 0 | 22.59 | 0 | 22.41 | 0 | 23.03 | 0 |
| 3.64 | 41.14 | 0 | 35.36 | 0 | 37.26 | 0 | 29.44 | 0 |

^a In ref. 33.

adsorption of F_4TCNQ , PTCDA, and tetracene, respectively. However, the bandgap of the MoS_2 remains the direct bandgap nature after the adsorption of the organic molecules.

The change of the lattice constant modifies the pressure applied to the system. The details of the bandgap and the pressure are described in Table 4 and visualized in Fig. 6. We found that the bandgap behavior of $\text{MoS}_2/\text{tetracene}$ is similar to

that of the monolayer MoS_2 , which exhibits a concave-downward curve with the maximum bandgap of 0.87 and 1.80 eV found at the pressure of -7.78 and -10.69 GPa for the $\text{MoS}_2/\text{tetracene}$ and monolayer MoS_2 , respectively. The concave-downward curve for the bandgap *versus* the pressure for the MoS_2 system was found to be in good agreement with experiment,³⁵ while that for the $\text{MoS}_2/\text{tetracene}$ is similar to that of an n-type semiconductor, the MoS_2/PEI interface, in the previous study.^{33,36} There is a little difference in the behavior of the bandgap *versus* the pressure for $\text{MoS}_2/\text{F}_4\text{TCNQ}$ and $\text{MoS}_2/\text{PTCDA}$ compared to that of the monolayer MoS_2 . That is the bandgap somehow linearly increases to a maximum value and then decreases with more positive pressures. The maximum value is 0.36 and 1.43 eV at the zero pressure for $\text{MoS}_2/\text{F}_4\text{TCNQ}$ and $\text{MoS}_2/\text{PTCDA}$, respectively. We have to impress that $\text{MoS}_2/\text{F}_4\text{TCNQ}$ and $\text{MoS}_2/\text{PTCDA}$ are the p-type semiconductors, which are different from the n-type of the $\text{MoS}_2/\text{tetracene}$. The monolayer MoS_2 , $\text{MoS}_2/\text{F}_4\text{TCNQ}$, $\text{MoS}_2/\text{PTCDA}$, and $\text{MoS}_2/\text{tetracene}$ were found to be completely converted to the metal with the bandgap of 0 eV at the pressure of 24.95, 22.59, 22.41, and 23.03 GPa, respectively.

In a complex structure, the Bader point charge of an atom was determined in two steps: (1) calculating the charge by the Bader partition technique, and (2) subtracting the charge obtained in step (1) to that of the neutral atom. In the pseudo-potential method of the DFT, one considers the contribution of valence electrons only. Table 5 presents the minus-plus signs as the loss and gain of charge, respectively. We found that F_4TCNQ and PTCDA accept while MoS_2 donates the charge. Contrastingly, the tetracene donates while MoS_2 gains the charge. These results are in a good correlation with the p-type doping nature of F_4TCNQ and PTCDA and the n-type doping of tetracene on the MoS_2 monolayer.

The electronic density of states (DOS) in Fig. 7a-c shows that the adsorption of F_4TCNQ , PTCDA, and tetracene contributes to the appearance of the new state coming from the p_z orbital of the organic molecules. As shown in Fig. 7d-f, the charge clouds of the atoms of the organic molecules clearly show the shape of p_z orbitals along the vertical direction, the vector c . The charge accumulation was found to more dominant on the F_4TCNQ and

Table 5 The point charge (in the unit of e) of the $\text{MoS}_2/\text{F}_4\text{TCNQ}$, $\text{MoS}_2/\text{PTCDA}$, and $\text{MoS}_2/\text{tetracene}$ systems

| $\text{MoS}_2/\text{F}_4\text{TCNQ}$ | | |
|--------------------------------------|----------------|-------------------------|
| P (GPa) | MoS_2 | F_4TCNQ |
| -57.93 | -0.226 | +0.226 |
| -25.03 | -0.098 | +0.098 |
| 0 | -0.073 | +0.073 |
| 12.21 | -0.144 | +0.144 |
| 22.59 | -0.231 | +0.231 |
| $\text{MoS}_2/\text{PTCDA}$ | | |
| P (GPa) | MoS_2 | PTCDA |
| 23.03 | -0.015 | +0.015 |
| 29.44 | -0.017 | +0.017 |
| -20.74 | -0.019 | +0.019 |
| 0 | -0.020 | +0.020 |
| 12.57 | -0.021 | +0.021 |
| 22.41 | -0.025 | +0.025 |
| $\text{MoS}_2/\text{tetracene}$ | | |
| P (GPa) | MoS_2 | Tetracene |
| -56.61 | +0.062 | -0.062 |
| -35.46 | +0.060 | -0.060 |
| -22.88 | +0.052 | -0.052 |
| -7.78 | +0.045 | -0.045 |
| 0 | +0.048 | -0.048 |
| 11.68 | +0.050 | -0.050 |
| 23.03 | +0.103 | -0.103 |
| 29.44 | +0.363 | -0.363 |



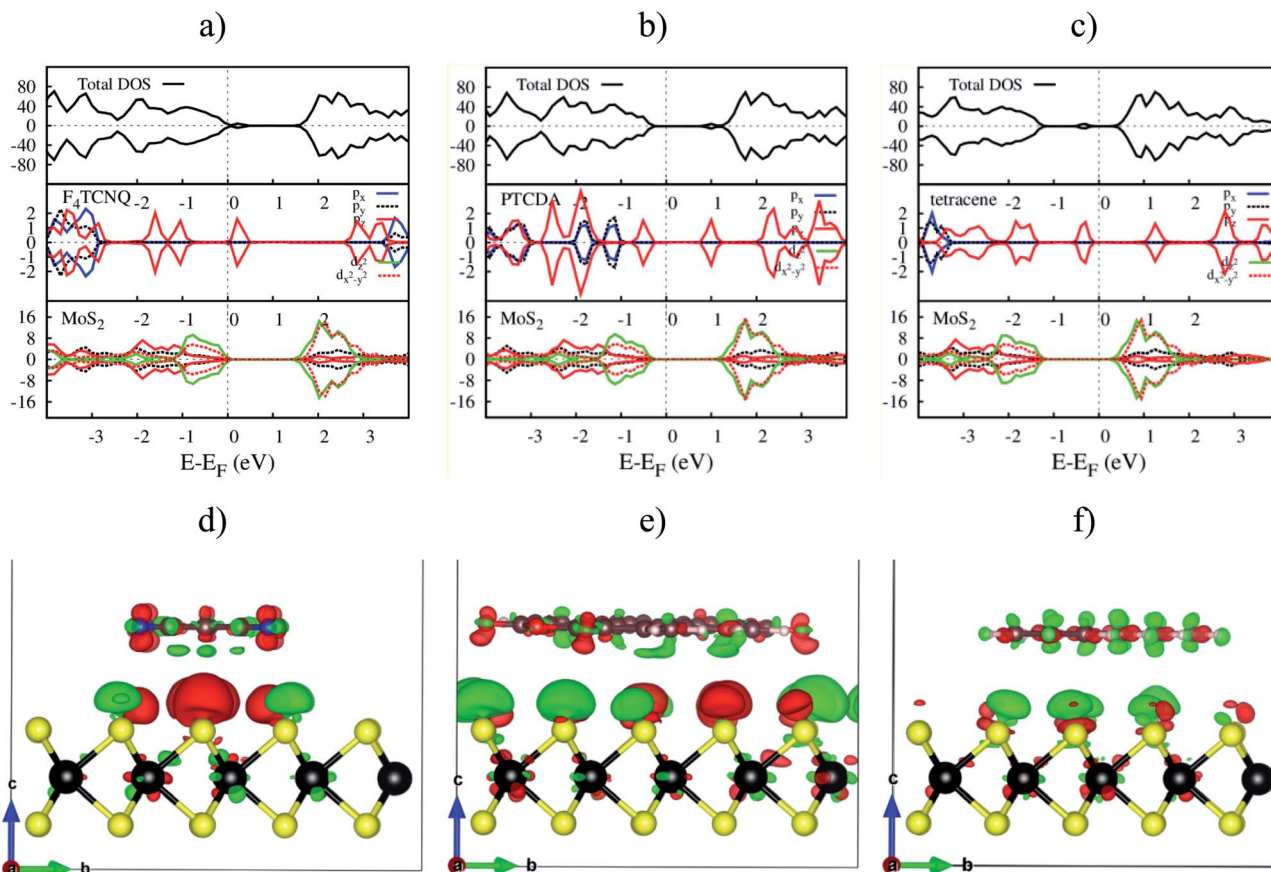


Fig. 7 The upper panel is the total and orbital-projected DOS. The bottom panel is the charge density difference at zero pressure. From left to right is for MoS₂/F₄TCNQ, MoS₂/PTCDA, and MoS₂/tetracene, respectively. Occupied and unoccupied states are presented in red and green in that order.

PTCDA, while the charge donation distributes more on tetracene. This result is in agreement with the above analysis about the Bader charge.

Fig. 8 shows the response of the total electronic density of states toward the influence of pressure. The p-type doping F₄TCNQ and PTCDA shift the valence band maximum of MoS₂

upward, while the n-type doping tetracene moves the conduction band minimum of MoS₂ downward near to the Fermi level. The variation of the position of the valence band maximum and conduction band minimum leads to modifying the bandgap of the systems.

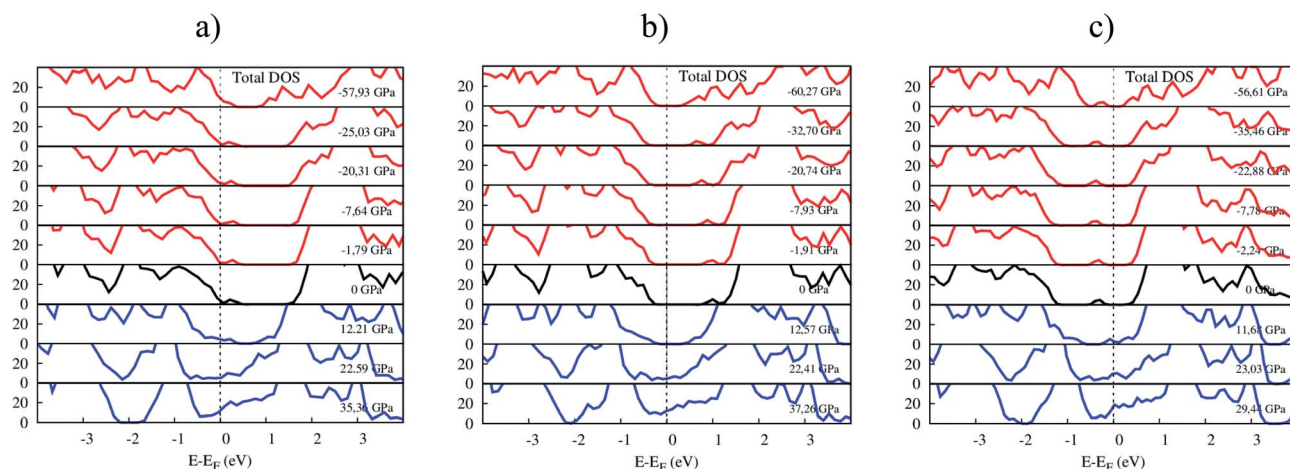


Fig. 8 The total DOS of (a) MoS₂/F₄TCNQ, (b) MoS₂/PTCDA, and (c) MoS₂/tetracene under pressure.



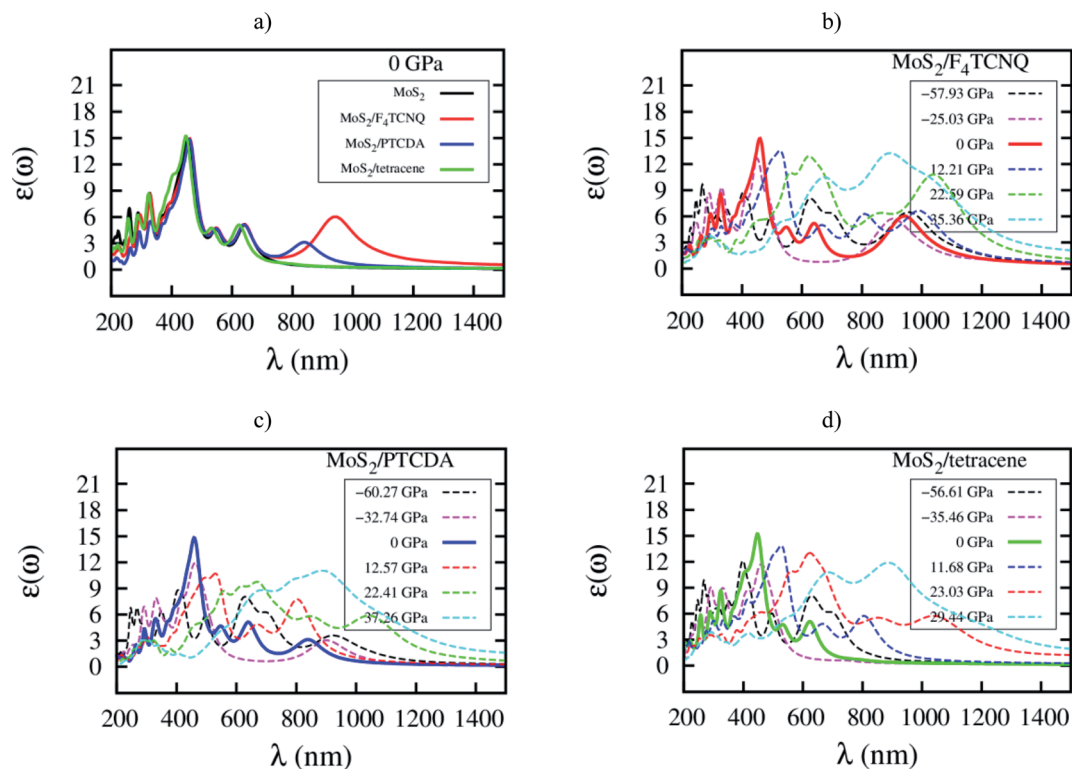


Fig. 9 Imaginary part of dielectric function $\epsilon(\omega)$ versus wavelength λ for (a) the systems at zero pressure, (b) $\text{MoS}_2/\text{F}_4\text{TCNQ}$, (c) $\text{MoS}_2/\text{PTCDA}$, and (d) $\text{MoS}_2/\text{tetracene}$ under pressure.

3.3. Optical properties

Here, we elucidate the influences of the organic molecular adsorption on the optical properties of the monolayer MoS_2 . The imaginary part of the frequency-dependent dielectric function of the MoS_2 , $\text{MoS}_2/\text{F}_4\text{TCNQ}$, $\text{MoS}_2/\text{PTCDA}$, and $\text{MoS}_2/\text{tetracene}$ in the independent-particle approximation including local field effects is presented in Fig. 9. After that, optical parameters as listed in Table 6 can be obtained in two steps: (1)

determining the wavelength λ and the intensity $\epsilon(\omega)$ at the maximum peak of the dielectric function, check Fig. 9, (2) calculating the corresponding photon energy $E_p = hc/\lambda$. At zero pressure, we found in Fig. 9a that the optical spectrum of the $\text{MoS}_2/\text{F}_4\text{TCNQ}$, $\text{MoS}_2/\text{PTCDA}$, and $\text{MoS}_2/\text{tetracene}$ systems has the maximum peak at almost the same position as that of the monolayer MoS_2 , which is at about 450 nm. The result indicates that these systems can emit and absorb blue light.^{29,37} The optical spectrum of the $\text{MoS}_2/\text{tetracene}$ has almost the same

Table 6 The wavelength and dielectric function at the maximum intensity of optical spectrum

| | | | | | | | |
|--------------------------------------|-------------------------|---------------|---------------|----------|--------------|--------------|--------------|
| MoS_2 (ref. 33) | P (GPa) | −56.18 | −32.44 | 0 | 10.13 | 24.95 | 41.14 |
| | E_p (eV) ^a | 4.66 | 2.60 | 2.73 | 2.39 | 2.00 | 1.42 |
| | λ (nm) | 266 | 477 | 453 | 521 | 621 | 873 |
| | $\epsilon(\omega)$ | 11.06 | 11.58 | 14.88 | 13.36 | 13.18 | 12.06 |
| $\text{MoS}_2/\text{F}_4\text{TCNQ}$ | P (GPa) | −57.93 | −25.03 | 0 | 12.21 | 22.59 | 35.36 |
| | E_p (eV) ^a | 4.62 | 2.75 | 2.69 | 2.36 | 1.99 | 1.38 |
| | λ (nm) | 268 | 451 | 461 | 526 | 624 | 896 |
| | $\epsilon(\omega)$ | 9.65 | 12.66 | 14.95 | 13.54 | 12.92 | 13.22 |
| $\text{MoS}_2/\text{PTCDA}$ | P (GPa) | −60.27 | −32.74 | 0 | 12.57 | 22.41 | 37.26 |
| | E_p (eV) ^a | 3.06 | 2.67 | 2.71 | 2.34 | 1.86 | 1.39 |
| | λ (nm) | 405 | 463 | 458 | 529 | 668 | 889 |
| | $\epsilon(\omega)$ | 8.82 | 11.95 | 14.82 | 10.72 | 9.76 | 11.05 |
| $\text{MoS}_2/\text{tetracene}$ | P (GPa) | −56.61 | −35.46 | 0 | 11.68 | 23.03 | 29.44 |
| | E_p (eV) ^a | 3.11 | 2.69 | 2.77 | 2.36 | 1.99 | 1.40 |
| | λ (nm) | 398 | 461 | 447 | 526 | 623 | 886 |
| | $\epsilon(\omega)$ | 12.11 | 11.72 | 15.21 | 13.85 | 13.03 | 11.90 |

^a $E_p = hc/\lambda$ is the photon energy, λ is the photon wavelength, h is Planck constant, and c is the speed of light in vacuum.



behavior as the monolayer MoS₂ with a little modification at short wavelengths around 300 nm. Contrastingly, the MoS₂/F₄TCNQ and MoS₂/PTCDA exhibits an additional peak at 950 and 850 nm, respectively. It is necessary to remind that the MoS₂/F₄TCNQ and MoS₂/PTCDA are p-type, while the MoS₂/tetracene is an n-type semiconductor. The behavior of the optical spectrum of the MoS₂/tetracene was found to be similar to that of the n-type doping of MoS₂ with PEI.³³ Therefore, the auxiliary peak at a longer wavelength was only found for the monolayer MoS₂ with the p-type doping.⁵ Furthermore, as shown in Fig. 9b–d, the intensity of the main optical peak at non-zero pressures was suppressed compared to that at 0 GPa.

4. Conclusion

This work investigated the effects of the organic molecular adsorption on the physical properties of the monolayer MoS₂ by the DFT calculations. The results have proved that the adsorption of F₄TCNQ, PTCDA, and tetracene on MoS₂ is physisorption. The organic molecular adsorption reduces the direct bandgap of the monolayer MoS₂ to 0.36, 1.43, and 0.72 eV, respectively. The main cause is due to the emergence of the new energy level at the conduction band minimum for MoS₂/F₄TCNQ and MoS₂/PTCDA, and at the valence band maximum for MoS₂/tetracene, by the p_z orbitals of the adsorbates. Under pressure, the bandgap of the MoS₂/F₄TCNQ, MoS₂/PTCDA, and MoS₂/tetracene systems reaches the maximum value of 0.36, 1.43, and 0.87 eV, respectively. Whilst, it becomes 0 eV implying the transition to the metal at the tensile pressure of 22.59, 22.41, and 23.03 GPa in that order. The adsorption of tetracene changes the optical peak structure of the monolayer MoS₂ at the ultraviolet region around 300 nm; however, the F₄TCNQ and PTCDA adsorption generate an auxiliary peak at the long wavelengths.

Conflicts of interest

There are no conflicts of interest to declare.

Acknowledgements

This research is funded by Ho Chi Minh City University of Technology (HCMUT), VNU-HCM, under grant number BK-SDH-2021-1680479.

References

- 1 B. Radisavljevic, A. Radenovic, J. Brivio, V. Giacometti and A. Kis, Single-layer MoS₂ transistors, *Nat. Nanotechnol.*, 2011, **6**, 147–150.
- 2 A. Splendiani, L. Sun, Y. Zhang, T. Li, J. Kim, C.-Y. Chim, G. Galli and F. Wang, Emerging Photoluminescence in Monolayer MoS₂, *Nano Lett.*, 2010, **10**, 1271.
- 3 K. F. Mak, C. Lee, J. Hone, J. Shan and T. F. Heinz, Atomically thin MoS₂: a new direct-gap semiconductor, *Phys. Rev. Lett.*, 2010, **105**, 136805.
- 4 M. Chhowalla, H. S. Shin, G. Eda, L.-J. Li, K. P. Loh and H. Zhang, The chemistry of two-dimensional layered transition metal dichalcogenide nanosheets, *Nat. Chem.*, 2013, **5**(4), 263–275.
- 5 Y. Jing, X. Tan, Z. Zhou and P. Shen, Tuning electronic and optical properties of MoS₂ monolayer *via* molecular charge transfer, *J. Mater. Chem. A*, 2014, **2**, 16892–16897.
- 6 W. Chen, S. Chen, D. C. Qi, X. Y. Gao and A. T. Wee, Surface transfer p-type doping of epitaxial graphene, *J. Am. Chem. Soc.*, 2007, **129**(34), 10418–10422.
- 7 Y. Du, H. Liu, A. T. Neal, M. Si and P. D. Ye, Molecular Doping of Multilayer MoS₂ Field-Effect Transistors: Reduction in Sheet and Contact Resistances, *IEEE Electron Device Lett.*, 2013, 0741–3106.
- 8 H. Huang, Y. Huang, S. Wang, M. Zhu, H. Xie, L. Zhang, X. Zheng, Q. Xie, D. Niu and Y. Gao, Van Der Waals Heterostructures between Small Organic Molecules and Layered Substrates, *Crystals*, 2016, **6**, 113.
- 9 Q. Huy Thi, H. Kim, J. Zhao and T. Hue Ly, Coating two-dimensional MoS₂ with polymer creates a corrosive non-uniform interface, *npj 2D Mater. Appl.*, 2018, **2**, 34.
- 10 H. Pinto, R. Jones, J. P. Goss and P. R. Briddon, p-type doping of graphene with F₄TCNQ, *J. Phys.: Condens. Matter*, 2009, **21**, 402001.
- 11 S. Mouri, Y. Miyauchi and K. Matsuda, Tunable Photoluminescence of Monolayer MoS₂ *via* Chemical Doping, *Nano Lett.*, 2013, **13**(12), 5944–5948.
- 12 P. Hu, J. Ye, X. He, K. Du, K. K. Zhang, X. Wang, Q. Xiong, Z. Liu, H. Jiang and C. Kloc, Control of Radiative Exciton Recombination by Charge Transfer Induced Surface Dipoles in MoS₂ and WS₂ Monolayers, *Sci. Rep.*, 2016, **6**, 24105.
- 13 J. Wang, Z. Ji, G. Yang, X. Chuai, F. Liu, Z. Zhou, C. Lu, W. Wei, X. Shi, J. Niu, L. Wang, H. Wang, J. Chen, N. Lu, C. Jiang, L. Li and M. Liu, Charge Transfer within the F₄TCNQ-MoS₂ van der Waals Interface: Toward Electrical Properties Tuning and Gas Sensing Application, *Adv. Funct. Mater.*, 2018, **28**(51), 1806244.
- 14 T. Ogawa, K. Kuwamoto, S. Isoda, T. Kobayashi and N. Karl, 3,4,9,10-Perylenetetra-carboxylic dianhydride (PTCDA) by electron crystallography, *Acta Crystallogr., Sect. B: Struct. Sci.*, 1999, **55**, 123–130.
- 15 S. Heutz, A. J. Ferguson, G. Rumbles and T. S. Jones, Morphology, structure and photophysics of thin films of perylene-3,4,9,10-tetracarboxylic dianhydride, *Org. Electron.*, 2002, **3**, 119–127.
- 16 Y. Han, W. Ning, H. Du, J. Yang, N. Wang, L. Cao, F. Li, F. Zhang, F. Xu and M. Tian, Preparation, Optical and Electrical Properties of PTCDA Nanostructures, *Nanoscale*, 2015, **7**, 17116–17121.
- 17 M. R. Habib, H. Li, Y. Kong, T. Liang, S. M. Obaidulla, S. Xie, S. Wang, X. Ma, H. Su and M. Xu, Tunable Photoluminescence in van der Waals Heterojunction Built from MoS₂ Monolayer and PTCDA Organic Semiconductor, *Nanoscale*, 2018, **10**, 16107–16115.
- 18 S. Wang, C. Chen, Z. Yu, Y. He, X. Chen, Q. Wan, Y. Shi, D. W. Zhang, H. Zhou, X. Wang and P. Zhou, A MoS₂/



- PTCDA Hybrid Heterojunction Synapse with Efficient Photoelectric Dual Modulation and Versatility, *Adv. Mater.*, 2018, **31**(3), 1806227.
- 19 L. Daukiya, J. Seibel and S. D. Feyter, Chemical modification of 2D materials using molecules and assemblies of molecules, *Adv. Phys.*, 2019, **4**(1), 1625723.
- 20 R. W. I. de Boer, T. M. Klapwijk and A. F. Morpurgo, Field-effect transistors on tetracene single crystals, *Appl. Phys. Lett.*, 2003, **83**, 4345.
- 21 H. J. Park, C.-J. Park, J. Y. Kim, M. S. Kim, J. Kim and J. Joo, Hybrid Characteristics of MoS₂ Monolayer with Organic Semiconducting Tetracene and Application to Anti-Ambipolar Field Effect Transistor, *ACS Appl. Mater. Interfaces*, 2018, **10**(38), 32556–32566.
- 22 G. Kresse and J. Hafner, *Ab initio* molecular dynamics for open-shell transition metals, *Phys. Rev. B: Condens. Matter Mater. Phys.*, 1993, **48**, 13115–13118.
- 23 G. Kresse and J. Hafner, *Ab initio* molecular-dynamics simulation of the liquid-metal–amorphous-semiconductor transition in germanium, *Phys. Rev. B: Condens. Matter Mater. Phys.*, 1994, **49**, 14251–14269.
- 24 G. Kresse and J. Furthmuller, Efficient iterative schemes for *ab initio* total-energy calculations using a plane-wave basis set, *Phys. Rev. B: Condens. Matter Mater. Phys.*, 1996, **54**, 11169–11186.
- 25 P. E. Blochl, Projector augmented-wave method, *Phys. Rev. B: Condens. Matter Mater. Phys.*, 1994, **50**, 17953.
- 26 G. Kresse and J. Joubert, From ultrasoft pseudopotentials to the projector augmented-wave method, *Phys. Rev. B: Condens. Matter Mater. Phys.*, 1999, **59**, 1758.
- 27 J. P. Perdew, J. A. Chevary, S. H. Vosko, K. A. Jackson, M. R. Pederson, D. J. Singh and C. Fiolhais, Atoms, molecules, solids, and surfaces: applications of the generalized gradient approximation for exchange and correlation, *Phys. Rev. B: Condens. Matter Mater. Phys.*, 1992, **46**, 6671.
- 28 J. P. Perdew, K. Burke and M. Ernzerhof, Generalized Gradient Approximation Made Simple, *Phys. Rev. Lett.*, 1996, **77**, 3865.
- 29 Y. Li, Y.-L. Li, C. M. Araujo, W. Luo and R. Ahuja, Single-layer MoS₂ as an efficient photocatalyst, *Catal.: Sci. Technol.*, 2013, **3**, 2214.
- 30 H. J. Monkhorst and J. D. Pack, Special points for Brillouin zone integrations, *Phys. Rev. B: Solid State*, 1976, **13**, 5188–5192.
- 31 J. Shang, L. Zhang, X. Cheng and F. Zhai, Pressure induced effects on the electronic and optical properties of MoS₂, *Solid State Commun.*, 2015, **219**, 33–38.
- 32 L. J. Kong, G. H. Liu and L. Qiang, Electronic and optical properties of O-doped monolayer MoS₂, *Comput. Mater. Sci.*, 2016, **111**, 416–423.
- 33 O. K. Le, V. Chihaiia, M.-P. Pham-Ho and D. N. Son, Electronic and optical properties of monolayer MoS₂ under the influence of polyethyleneimine adsorption and pressure, *RSC Adv.*, 2020, **10**, 4201–4210.
- 34 M. M. Ugeda, A. J. Bradley, *et al.*, Giant bandgap renormalization and excitonic effects in a monolayer transition metal dichalcogenide semiconductor, *Nat. Mater.*, 2014, **13**, 1091–1095.
- 35 X. Cheng, Y. Li, J. Shang, C. Hu, Y. Ren, M. Liu and Z. Qi, Thickness-dependent phase transition and optical behavior of MoS₂ films under high pressure, *Nano Res.*, 2018, **11**, 855–863.
- 36 V. K. Dien, O. K. Le, V. Chihaiia, M. P. Pham-Ho and D. N. Son, Monolayer transition-metal dichalcogenides with polyethyleneimine adsorption, *J. Comput. Electron.*, 2021, DOI: 10.1007/s10825-020-01630-2.
- 37 Z. Yin, H. Li, H. Li, L. Jiang, Y. Shi, Y. Sun, G. Lu, Q. Zhang, X. Chen and H. Zhang, Single-Layer MoS₂ Phototransistors, *ACS Nano*, 2011, **6**, 74–80.

